Optimization of an Indirect Evaporative Cooler in Liquid Desiccant and Evaporative Cooling-assisted 100% Outdoor Air Systems

H.J. Kim, S.J. Lee and J.W.Jeong*

Department of Architectural Engineering, College of Engineering, Hanyang University, Seoul, 133-791, Korea,

ABSTRACT

The main purpose of this study is to propose the optimal geometry for a cross-flow indirect evaporative cooling system and evaluate its energy-saving potential when applying a liquid desiccant and evaporative cooling-assisted 100% outdoor air system. The optimization of the indirect evaporative cooling system was conducted with a numerical model that was validated with empirical data. The optimal geometry was determined considering the system coefficient of performance and supply air temperature through multi-objective optimization using a genetic algorithm. The cooling performance of the optimized indirect evaporative cooling system applied with the liquid desiccant system was compared with that of the base indirect evaporative cooling system. To evaluate the further energy-saving potential of the optimal indirect evaporative cooling system in an overall system configuration during the cooling season, energy consumption of the liquid desiccant and evaporative cooling-assisted 100% outdoor air systems was calculated in the cases of optimal and base indirect evaporative cooling system applications.

KEYWORDS

Optimization, Indirect evaporative cooler, Optimum design, liquid desiccant system

INTRODUCTION

Indirect evaporative cooling systems have been playing a key role in conserving the energy consumption of the heating, ventilating, and air conditioning (HVAC) system in buildings by utilizing the vaporization process of water. Unlike a conventional direct evaporative cooler (DEC) that supplies water and air into the same channels, IEC separates process air (i.e., primary air) from water with dry channels (i.e., primary channels) and wet channels (i.e., secondary channels) so that it can indirectly cool the process air without any humidification. The sensible cooling effect of the IEC can be enhanced when it is supplied with the dry primary air or the secondary air that shows low wet-bulb temperature. In this sense, a liquid desiccant (LD) system that dehumidifies the process air is essential for improving the performance of the IEC as well as controlling the humidity level of the conditioned space. (Woods 2013,

* Corresponding author email: jjwarc@hanyang.ac.kr

Riangvilaikul 2010). The IEC decoupled with LD can reduce the system load of the conventional VAV that consumes excessive energy for controlling humidity and the temperature of the supply air, especially when applied in an 100% outdoor air system that can supply room air to the secondary channels of the IEC to enhance its sensible cooling effect. In such system configuration, optimizing the geometry and the process air condition of IEC unit can even enhance the overall system cooling performance. The purpose of this paper is to optimize the geometry and the properties of the primary air of the IEC to enhance its cooling performance for an LD and an evaporative cooling-assisted 100% outdoor air system. The supply air temperature and the coefficient of performance of the IEC unit are selected as the objective function of the optimization. Then, an energy simulation was conducted to evaluate the contribution of optimized IEC on the LD and evaporative cooling-assisted 100% outdoor air system.

NUMERICAL MODEL

Heat and mass transfer model

The governing equations of the IEC are derived from the heat and mass transfer between the primary channel and the neighboring secondary channel. From the energy balance equation, the sensible and latent heat transfer equations can be derived as Equations (1) and (2).

$$\frac{dT_p}{dA} = -\frac{h_{p-w}}{m_p c_{p,ma}}\left(T_p - T_w\right) \tag{1}$$

$$\frac{d\omega_s}{dA} = \frac{h_m}{m_p}\left(\omega_{sat,w} - \omega_s\right) \tag{2}$$

Where dT_p is the differential primary air temperature (°C); dA is the differential area (m^2); $h_{p\text{-}w}$ is the heat transfer coefficient (w/m^2K) between the primary channel, secondary channel and water film; T_p is the primary air outlet temperature (°C); T_w is the temperature of the water film (°C); and c_p is the specific heat of the process air (kJ/kgK). From the energy balance equations in the secondary channels, the following governing equations are derived.

$$\frac{dT_s}{dA} = \frac{h_s}{m_s c_{p,ma}}\left(T_w - T_s\right) \tag{3}$$

$$\frac{d\omega_s}{dA} = \frac{h_m}{m_s}\left(\omega_{sat,w} - \omega_s\right) \tag{4}$$

Here, h_s, T_s and m_s represent enthalpy (kJ/kg), temperature (°C), and mass flow rate (kg/s) of the secondary air stream, respectively. Also, h_m and $\omega_{sat,w}$ represent the mass transfer coefficient (kg/m^2K) and the saturation humidity ratio of the wet channel (kg/kg), respectively. Equation (5) is derived from the fact that the sensible and latent heat transferred from the primary channel equals that of the secondary channel.

$$h_{p-w}(T_p - T_w)dA = h_s(T_w - T_s)dA + (i_{vap@0} + c_{p,v}T_s)h_m(\omega_{sat,w} - \omega_s)dA \quad (5)$$

$I_{vap@0}$ and $c_{p,v}$ are the latent heat of vaporization at 0°C (kJ/kg) and specific heat of water vapor (kJ/kgK), respectively. The finite difference model was used for analyzing the governing equations of the IEC unit (Fig. 1). The established numerical model was validated with the IEC experimental data obtained in a previous experiment (Kim 2016). The discrepancies between the primary air outlet temperature of the experimental data and the numerical model was within 3%.

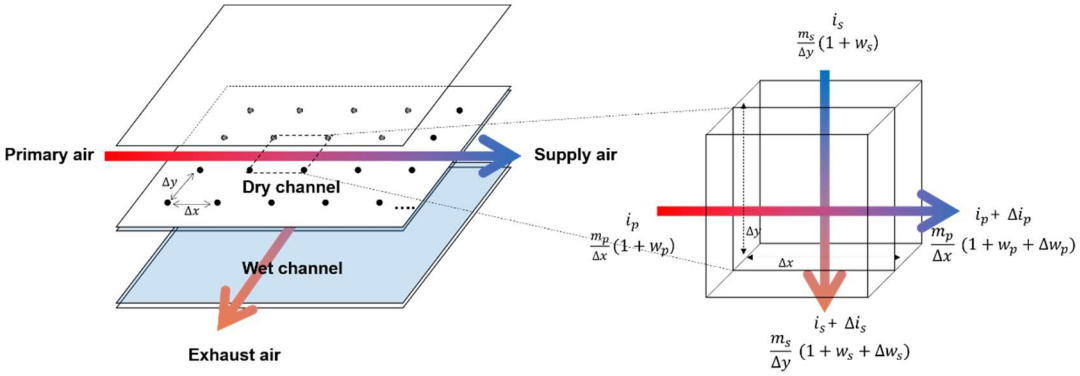

Figure 1. *The differential representation of the numerical model*

MULTI-OBJECTIVE OPTIMIZATION

Objective functions

The optimization was performed to enhance the system efficiency and the cooling performance of the IEC that is applied with LD. To optimize the IEC that supplies dehumidified air into the primary channel and room air into the secondary channel, the condition of the primary and secondary air inlet temperature and humidity was fixed as follows: a dry-bulb temperature (DBT) of 30 °C and humidity ratio of 8.1 g/kg for the primary air, and a DBT 24.5 °C and humidity ratio of 10 g/kg for the secondary air. Under such conditions, the optimization was performed to find the optimum geometry and air velocity of IEC that enhance the system cooling performance. The variable range for optimization is specified in Table 1. The supply air temperature and the coefficient of performance (COP) were selected as objective functions. The optimal solutions that minimize the supply air temperature of the IEC and the inverse of the COP (COP^{-1}) were selected through the multi-objective genetic algorithm (GA) function in MATLAB (MathWorks, 2014).

The previously defined numerical model was utilized for deriving the regression model of the primary air outlet temperature (Eq. 6). The regression model was defined with 10 parameters including the geometry of the IEC unit and the properties of the primary and the secondary air stream: primary channel length (L_x (m)), secondary channel length to primary channel length ratio (LH (m)), channel gap of the primary channel and secondary channel (tp (m), ts (m)), primary air to secondary air mass flow rate ratio (r), temperature (°C) and the humidity ratio (kg/kg) of primary and secondary channels

(T_p, w_p, T_s, w_s), and the velocity of the primary air (v_p (m/s)). The variables in the regression model had the same range of optimization parameters with a temperature range of 25°C to 30°C and humidity ratio range of 7g/kg to 20g/kg. Within the variable range, 96 sets of variables were randomly selected through the Model browser in MATLAB (MathWorks, 2014), and regressed to the supply air temperature calculated from the IEC numerical model. The R^2 value of the regression model was 0.98.

***Table 1**. The range of the optimization parameters*

	Minimum	*Maximum*
Primary channel length (L_x)	0.3 m	1.5 m
H/L	0.5	2
Primary channel gap (tp)	0.002 m	0.006 m
Secondary channel gap (ts)	0.002 m	0.006 m
Primary air velocity	0.5 m/s	5 m/s
Ratio of the secondary air and primary air mass flow rate (r)	0.3	1

$$T_{iec} = \begin{pmatrix} 5.075 - 4.558 \cdot L_x + 2.011 \cdot LH - 194.283 \cdot tp + 236.393 \cdot ts - 0.181 \cdot T_{pi} + 75.051 \cdot W_{pi} \\ +0.411 \cdot T_{si} + 1008.091 \cdot W_{si} - 0.048 \cdot v_p - 6.958 \cdot r - 0.264 \cdot L_x \cdot T_{pi} - 76.149 \cdot L_x \cdot W_{pi} + 0.133 \cdot L_x \cdot T_{si} \\ +169.418 \cdot L_x \cdot W_{si} - 1.473 \cdot L_x \cdot r + 220.665 \cdot LH \cdot ts - 0.066 \cdot LH \cdot T_{si} - 53.608 \cdot LH \cdot W_{si} \\ +118.004 \cdot tp \cdot T_{pi} - 23.379 \cdot tp \cdot T_{si} - 80550.945 \cdot tp \cdot W_{si} + 50.801 \cdot tp \cdot v_p + 19.508 \cdot ts \cdot T_{pi} \\ -23963.651 \cdot ts \cdot W_{pi} + 0.049 \cdot T_{pi} \cdot v_p + 6867.833 \cdot W_{pi} \cdot W_{si} - 10.589 \cdot T_{si} \cdot W_{si} - 0.012 \cdot T_{si} \cdot v_p \\ -25.729 \cdot W_{si} \cdot v_p + 3.097 \cdot L_x^2 - 118595.403 \cdot tp^2 - 83246.613 \cdot ts^2 - 0.049 \cdot v_p^2 + 5.592 \cdot r^2 \end{pmatrix} \quad (6)$$

The COP of the IEC unit was evaluated as the ratio of the cooling capacity (Q_{cc} (W)) and the power of the supply fan (P (W)) (Eqs. 7-10). The cooling capacity of the IEC is expressed using the mass flow rate (m_{pi} (kg/s)) and specific heat (cp (kJ/kgK)) of the primary air, as well as the temperature difference (°C) between the primary air outlet (T_{po}) and the inlet temperature (T_{pi}). The core pressure drop of the primary channels (Δp (Pa)) in IEC was calculated considering the pressure loss due to the entrance effect, momentum effect, core friction, and exit effect (Lee 2010). The efficiency of the fan (ε_{fan}) was set to 60%.

$$COP = \frac{Q_{cc}}{P} \quad (7)$$

$$Q_{cc} = m_{pi} c_p (T_{pi} - T_{po}) \quad (8)$$

$$\Delta p = \frac{(\rho_i \cdot v_p)^2}{2 \cdot \rho_i} \left(1 - \sigma^2 + K_c + 2 \cdot \left(\frac{\rho_i}{\rho_o} - 1 \right) + 4Fr \cdot \frac{L_x}{D_h} \cdot \rho_i \cdot \left(\frac{1}{\rho_i} + \frac{1}{\rho_o} \right) \cdot 0.5 - (1 - \sigma^2 - K_e) \cdot \left(\frac{\rho_i}{\rho_o} \right) \right) \quad (9)$$

$$P = \frac{\dot{V_{pi}} \Delta p}{\varepsilon_{fan}} \quad (10)$$

Decision making in optimal solutions

After finding the set of optimal solutions, a decision making process was required to select a single optimum solution among 58 sets of optimal solutions that have a trade-off in their objective values. To find a single optimum solution, a multi-criteria decision making technique, specifically the reference point method, was used (Deb 2006). The advantage of the reference point method is that the engineers can select a single optimum point by reflecting their preference through the weight factor and reference point chosen by their own. One can find an optimum solution closest to the reference point by selecting the point that minimizes the weighted-sum of the objectives (Eq. 11). ω_i is the weight factor, $\bar{z}_i$ is the reference point, and f_i is the objective function. In this paper, the reference point of the Pareto-front was selected as a minimum value of the outputs of the objective functions, and a weight factor of 0.5 was applied to each objective function. The weighted sum of the distance between the solutions and the reference point was calculated based on the non-dimensional Pareto-front. After normalizing the values of the objective functions, the optimum point was found through the reference point method, as shown in Figure. 2.

$$\text{Minimize} \quad \max_{x \in S.} \sum_{i=1}^{2} [\omega_i (f_i(x) - \bar{z}_i)] \tag{11}$$

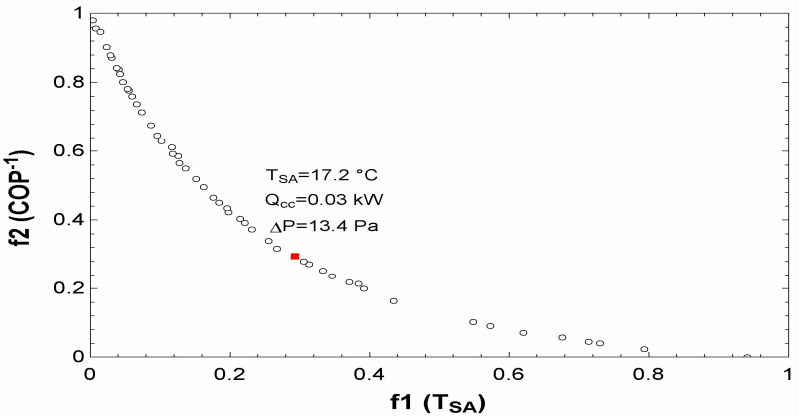

Figure 2. *Pareto-optimal solutions and final optimal point*

Optimum geometry of IEC

The optimum geometry of the IEC unit is specified in Table 2. The result showed that the cooling performance of IEC was optimized when applied with the longest primary channel length and the narrowest channel gap. Also, the low velocity of the primary air was key for optimizing the IEC.

Table 2. *The optimized geometry and primary air properties of the IEC*

parameter	*Results*
Primary channel length (L_x)	1.5 m
H/L	0.6
Primary channel gap (tp)	0.003 m
Secondary channel gap (ts)	0.002 m
Primary air velocity (v_p)	0.5 m/s
m_{si}/m_{pi} (=r)	1

SIMULATION OVERVIEW

The energy simulation was conducted to compare the performance of two IEC units applied with LD and a cooling coil for the summer season (June, July, August). As shown in Figure. 3, Case 1 illustrates the system applied with base IEC while Case 2 illustrates the system applied with the optimized IEC. The specification of two IEC units are described in Table 3. For energy simulation, the sensible and latent loads of the model building was simulated with the TRNSYS 17 program, and the performance of IEC, LD, and cooling coil was simulated with the commercial engineering equation solver (EES). The temperature and relative humidity of the room air was 25 °C and 50%, while that of the supply air was set to 15 °C and 80%. The outdoor air was first dehumidified by the LD, and then cooled by the IEC that sends room air into the secondary channels. Then, the process air that passed IEC was additionally cooled and dehumidified to the target supply air condition by passing the cooling coil. For LD system, the absorber model was referenced from the desiccant-enhanced evaporative air cooler (Woods 2013). The outlet humidity ratio of the liquid desiccant system was regressed to the experimental data using the following parameters: liquid to gas ratio, inlet temperature, humidity ratio, and the concentration of the liquid desiccant solution. The temperature of process air that passed IEC was predicted by using equation 6. For simulating the chiller energy consumption, the DOE2 electric air cooled chiller model was used (EnergyPlus 2016). In the energy simulation, the major difference between Case 1 and Case 2 was the IEC model, and the chiller energy required to condition the process air that passed the IEC unit. Therefore, the performances of the two system configurations were analyzed by comparing the temperature profile and the chiller energy consumption.

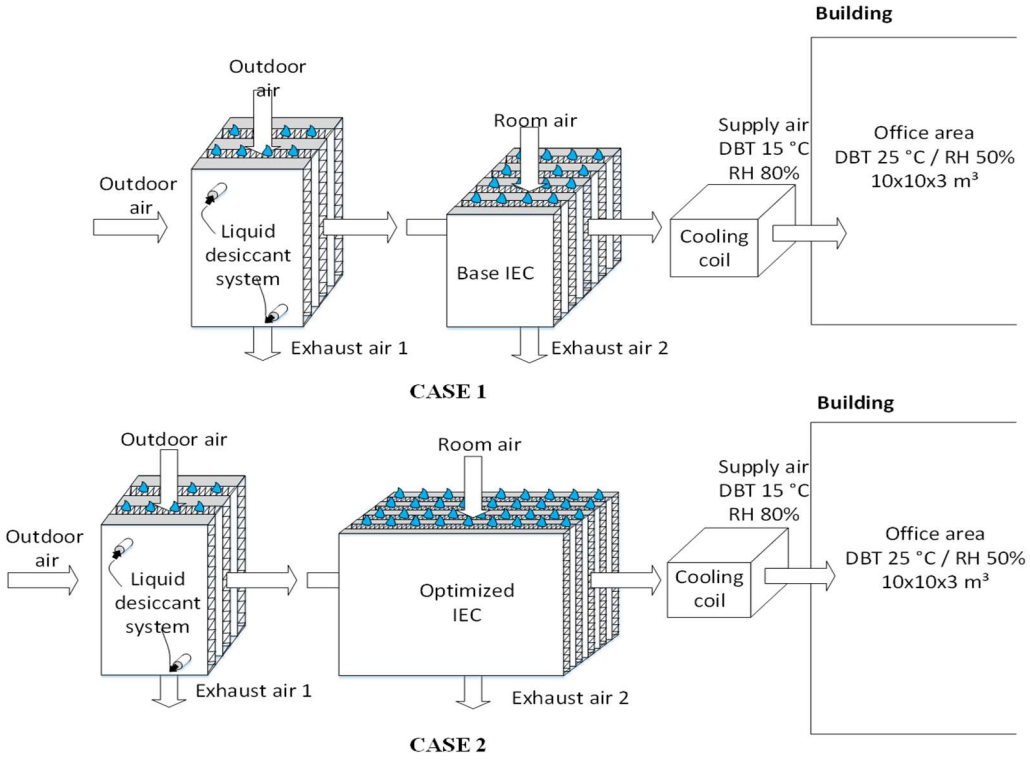

Figure 3. *Schematics of LD and IEC assisted 100% outdoor air system*

Table 3. *Specifications of the IEC unit in Case 1 and Case 2*

Parameter	*Base IEC*	*Optimized IEC*
Primary channel length (L_x)	0.38 m	1.5 m
H/L	1	0.6
Primary channel gap (tp)	0.005 m	0.003 m
Secondary channel gap (ts)	0.005 m	0.002 m
Number of channels	Primary: 38 Secondary: 38	Primary: 90 Secondary: 90

SIMULATION RESULTS

Performance of IEC applied with liquid desiccant

Figure 4 shows the temperature profile of process air in Case 1 and Case 2 during a peak summer day. In Case 1 and Case2, the outdoor air that was initially dehumidified by LD passed through each of IEC unit, and then it was conditioned by the cooling coil to meet the target supply air condition. While the base IEC unit in Case 1 failed to send the supply air below the temperature of 20°C, especially during 2-4 PM, the optimized IEC unit in Case 2 cooled the process air near to 17°C during whole office hours. The primary air face velocity as well as the geometry of the base IEC was responsible for the high cooling performance of the optimized IEC. Unlike the base IEC that had to condition the primary air flowing with the mean air velocity of 1.3m/s, the optimized IEC that conditioned the primary air flowing with the mean face velocity of 0.5m/s was able to increase the duration of the heat transfer. Moreover, the optimized IEC in Case 2 was able to show higher cooling effect than the base IEC in Case 1 due to its optimized channel gap size and the length of channels. The narrower channel gap and the longer dry and wet channels contributed to increasing the sensible cooling effect. Therefore, the energy simulation during the summer season showed that the optimized IEC in Case 2 contributed to reducing 70% more chiller energy consumption in the liquid desiccant and evaporative cooling-assisted 100% outdoor air system than the base IEC.

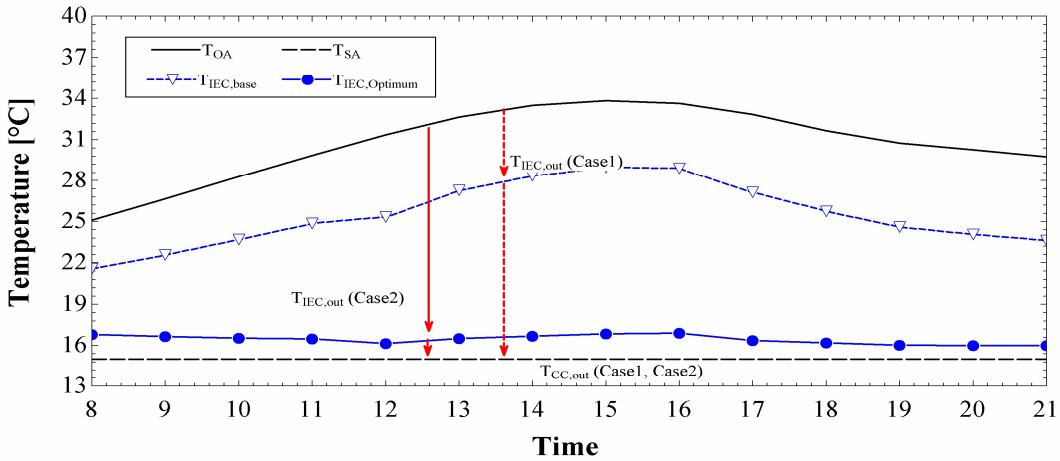

Figure 4. *Temperature profile of Case 1 and Case 2*

CONCLUSION AND DISCUSSION

The main purpose of this paper was to optimize the geometry of the IEC unit and the primary air properties to enhance the COP and cooling effect of the conventional cross flow type IEC. For optimization, the supply air temperature and the reverse value of the

COP were selected as objective functions for minimization. The regression model of the supply air temperature was derived from the data pool of the numerical model, and the system cooling capacity and supply fan energy consumption were utilized for evaluating the system COP. Then, an energy simulation was conducted to evaluate the contribution of optimized IEC on the liquid desiccant and evaporative cooling-assisted 100% outdoor air system. The results show that the optimized IEC was able to reduce the chiller energy consumption by approximately 45% compared to the system applied with the base IEC.

ACKNOWLEDGEMENTS

This work was supported by a National Research Foundation (NRF) grant (No. 2015R1A2A1A05001726) and a Korea Institute of Energy Technology Evaluation and Planning (KETEP) and the Ministry of Trade, Industry & Energy (MOTIE) of the Republic of Korea (No. 20164010200860).

REFERENCES

Alklaibi A. M. 2015. Experimental and theoretical investigation of internal two-stage evaporative cooler, Energy Converssion and Management, Vol 95, pp 140–148.

Cerci Y. 2003. A new ideal evaporative freezing cycle, International Journal of Heat and Mass Transfer, Vol 46, pp 2967–2974.

Deb K. and Sundar J. 2006. Reference Point Based Multi-Objective Optimization Using Evolutionary Algorithms, Genetic and Evolutionary Computation, Vol 1, pp 635–642.

EnergyPlus. 2015. EnergyPlus Engineering Reference: The Reference to EnergyPlus Calculations, US Department of Energy, https://energyplus.net/sites/all/modules/custom/nrel_custom/pdfs/pdfs_v8.5.0/EngineeringReference.pdf, last updated on 31 March 2016.

Kim H, Ham S, Yoon D, and Jeong J. 2016. Performance Evaluation of Two Cross Type Indirect Evaporative Air Coolers, *CLIMA 2016 - Proceedings of the 12th REHVA World Congress*, Vol. 2.

Lee H. 2010. *Thermal design: heat sinks, thermoelectrics, heat pipes, compact heat exchangers, and solar cells*, New Jersey: John Wiley & Sons Press.

MathWorks. 2014. Model-Based Calibration Toolbox ™ Model Browser User's Guide R 2015a, Version 4.8.1

Pescod D. 1979. A heat excanger for energy saving in an air-conditioning plant, ASHRAE Transactions, Vol 85, pp 238-251

Riangvilaikul B. and Kumar S. 2010. An experimental study of a novel dew point evaporative cooling system, Energy and Buildings, Vol 42, pp 637–644.

Woods J. Kozubal E. 2013. A desiccant-enhanced evaporative air conditioner: Numerical model and experiments, Energy Conversion and Management, Vol 65, pp 208–220.